Mechanisms of Propagation and Termination Reactions in Classical Heterogeneous Ziegler−Natta Catalytic Systems: A Nonlocal Density Functional Study

Luigi Cavallo,*,† Gaetano Guerra,‡ and Paolo Corradini†

Contribution from the Dipartimento di Chimica, Università di Napoli, Via Mezzocannone 4, I-80134 Naples, Italy, and Dipartimento di Chimica, Università di Salerno, Baronissi, I-84081 Salerno, Italy

Received July 31, 1997. Revised Manuscript Received December 1, 1997

Abstract: A nonlocal density functional study of ethylene polymerization with a model for the heterogeneous Ziegler−Natta catalyst is presented. We have considered the propagation as well as the termination reactions. In the absence of a coordinated olefin, the Ti−C (chain) σ bond does not occupy an octahedral coordination position but is oriented along an axis that is intermediate between the two octahedral coordination positions which are available. The propagation reaction occurs in a stepwise fashion, and the most favored mechanism requires a rearrangement of the growing chain out of the four-center transition-state plane. The insertion reaction is facilitated by a remarkable α-agostic interaction. The most favored termination reaction corresponds to the β-hydrogen transfer to the monomer. This reaction is favored relative to the C−H σ-bond activation of a coordinated monomer, as well as to the β-hydrogen transfer to the metal.

Introduction

It is well-known that polymerization of alkenes with heterogeneous Ziegler−Natta catalysts is one of the most important polymerization reactions.[1] However, despite the intense theoretical research activity that has centered around homogeneous Ziegler−Natta catalytic systems in the past decade,[2] very few efforts have been devoted to the clarification of the elementary steps that rule this reaction for the classical heterogeneous systems,[3] of overwhelming industrial relevance. One of the reasons is the complexity of the systems employed; the exact nature of the active center is not yet fully understood. Over the years, from simple $TiCl_3$ crystals,[4] the catalyst has evolved into the nowadays-used high-technology systems based on the use of magnesium dichloride as a support for $TiCl_4$.[5] After mechanical co-milling of $MgCl_2$ with $TiCl_4$ and an organic Lewis base (the so-called internal donor), the active polymerization sites are formed by treating the adsorbed $TiCl_4$ molecules with an alkylating reducing species, such as AlR_3, and a second electron donor (the so-called external donor).[6] The resulting catalytic system is of extreme chemical complexity. For these reasons, although a very important industrial target has been obtained, the intimate nature of the active sites is still poorly understood.

Despite these difficulties, Arlman and Cossee have proposed a widely accepted mechanism.[7] Arlman devised the presence of vacancies on the surface of the crystals,[7b] while Cossee modeled the active center as an octahedrally coordinated Ti atom.[7a] The metal is surrounded by four chlorine atoms which connect the Ti to the bulk of the crystal and an alkyl group which develops into the growing chain, while the last coordination position is occupied at each polymerization step by an incoming monomer molecule.

Some theoretical studies have been devoted to the clarification of the elementary steps,[3,8] but all the considered systems always concerned the insertion on a simple Ti−CH_3 bond. Moreover,

* E-mail: cavallo@chemna.dichi.unina.it.
† Università di Napoli.
‡ Università di Salerno.

(1) (a) Natta, G. *Nobel Lectures in Chemistry, 1963−1970*; Elsevier: Amsterdam, 1972; p 27. (b) Ziegler, K. *Nobel Lectures in Chemistry, 1963−1970*; Elsevier: Amsterdam, 1972; p 6. (c) Boor, J., Jr. *Ziegler−Natta Catalysts and Polymerizations*; Academic: New York, 1979. (d) Kissin, Y. V. *Isospecific Polymerization of Olefins*; Springer-Verlag: New York, 1985. (e) Tait, P. J. T.; Watkins, N. D. *Comprehensive Polymer Science*; Pergamon: New York, 1989; Vol. 4, p 533. (f) Albizzati, E.; Giannini, U.; Collina, G.; Noristi, L.; Resconi, L. In *Polypropylene Handbook*; Moore, E. P., Jr., Ed.; Hanser: New York, 1996; p 11.

(2) (a) Jolly, C. A.; Marynick, D. S. *J. Am. Chem. Soc.* **1989**, *111*, 7968. (b) Kuribayashi, H. K.; Koga, N.; Morokuma, K. *J. Am. Chem. Soc.* **1992**, *114*, 2359. (c) Castonguay, L. A.; Rappé, A. K. *J. Am. Chem. Soc.* **1992**, *114*, 5832. (d) Prosenc, M.; Janiak, C.; Brintzinger, H. H. *Organometallics* **1992**, *11*, 4036. (e) Woo, T.; Fan, L.; Ziegler, T. *Organometallics* **1994**, *13*, 432. (f) Sini, G.; Macgregor, S. A.; Eisenstein, O.; Teuben, J. H. *Organometallics* **1994**, *13*, 1049. (g) Weiss, H.; Ehrig, M.; Ahlrics, R. *J. Am. Chem. Soc.* **1994**, *116*, 4919. (h) Meier, R. J.; Doremaele, G. H. J. V.; Iarlori, S.; Buda, F. *J. Am. Chem. Soc.* **1994**, *116*, 7274. (i) Yoshida, T.; Koga, N.; Morokuma, K. *Organometallics* **1995**, *14*, 746. (j) Støvneng, J. A.; Rytter, E. *J. Organomet. Chem.* **1996**, *519*, 277. (k) Woo, T. K.; Margl, P. M.; Lohrenz, J. C. W.; Blöchl, P. E.; Ziegler, T. *J. Am. Chem. Soc.* **1996**, *118*, 13021.

(3) (a) Fujimoto, H.; Yamasaki, T.; Mizutani, H.; Koga, N. *J. Am. Chem. Soc.* **1985**, *107*, 6157. (b) Sakai, S. *J. Phys. Chem.* **1991**, *95*, 175. (c) Sakai, S. *J. Phys. Chem.* **1991**, *95*, 7089. (d) Novaro, O. *Int. J. Quantum Chem.* **1992**, *114*, 5832. (e) Sakai, S. *J. Phys. Chem.* **1994**, *98*, 12053. (f) Jensen, V. R.; Børve, K. J.; Ystens, M. *J. Am. Chem. Soc.* **1995**, *117*, 4109.

(4) (a) Ziegler, K. *Angew. Chem.* **1964**, *76*, 545. (b) Natta, G. *Chim. Ind. (Milan)* **1964**, *46*, 397. (c) Natta, G. *Science* **1965**, *147*, 261.

(5) Montedison, British Patent 1,286,867, 1968.

(6) Barbé, C.; Cecchin, G.; Noristi, L. *Adv. Polym. Sci.* **1987**, *81*, 1.

(7) (a) Cossee, P. *J. Catal.* **1964**, *3*, 80. (b) Arlman, E. J. *Proc. Int. Congr. Catal., 3rd* **1964**, *2*, 957. (c) Arlman, E. J.; Cossee, P. *J. Catal.* **1964**, *3*, 99.

(8) (a) Armstrong, D. R.; Perkins, P. G.; Stweart, J. J. P. *J. Chem. Soc., Dalton Trans.* **1972**, 1972. (b) Novaro, O.; Chow, S.; Magnouat, P. *J. Catal.* **1976**, *41*, 91. (c) Giunchi, G.; Clementi, E.; Ruiz-Vizcaya, M. E.; Novaro, O. *Chem. Phys. Lett.* **1977**, *49*, 8. (d) Novaro, O.; Blaisten-Barojas, E.; Clementi, E.; Giunchi, G.; Ruiz-Vizcaya, M. E. *J. Chem. Phys.* **1978**, *68*, 2337. (e) Fujimoto, H.; Yamasaki, T.; Mizutani, H.; Koga, N. *J. Am. Chem. Soc.* **1981**, *103*, 7452.

S0002-7863(97)02618-8 CCC: $15.00 © 1998 American Chemical Society
Published on Web 03/03/1998

Scheme 1

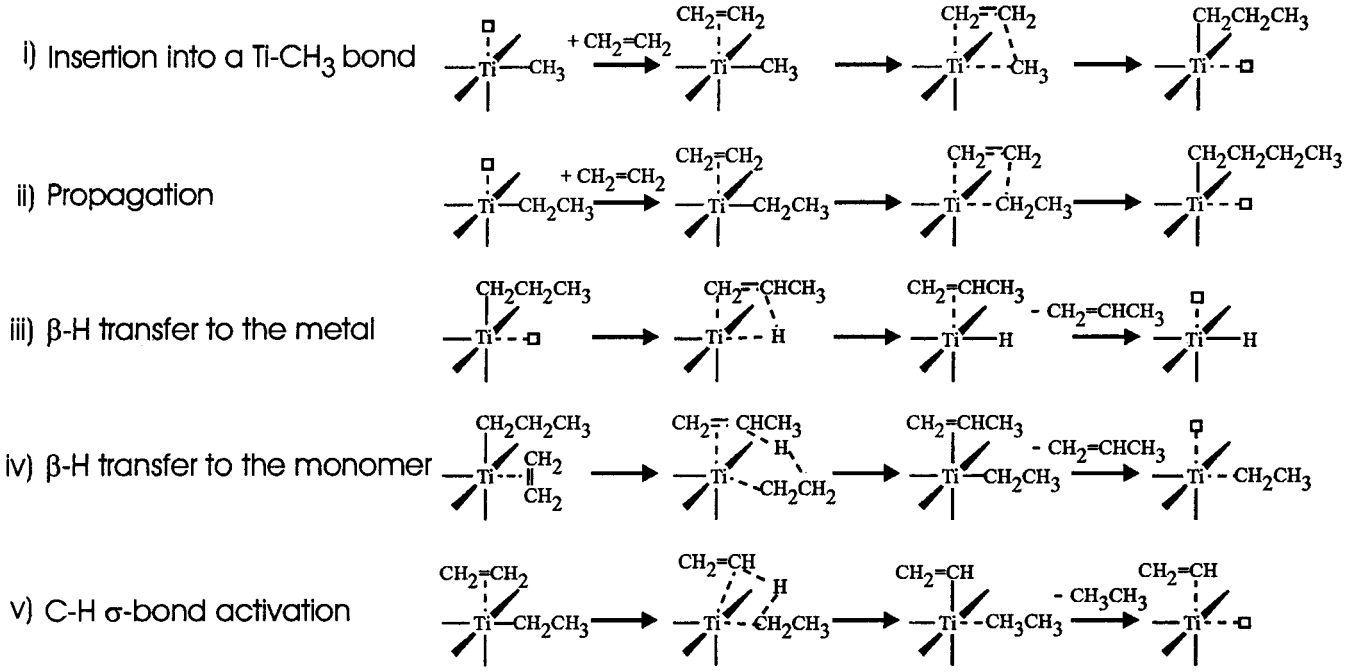

termination reactions have never been considered, and a consistent comparison of all these reactions is still lacking. Finally, in all the considered systems, the oxidation state of the Ti atom was chosen to be IV, while experimental results[9] suggest that the active species is a Ti atom in the oxidation state III.

For these reasons, in the wake of analogous density functional studies on the homogeneous systems performed by Ziegler and co-workers,[2e,k,10] we performed the present study to provide a consistent picture of the reactions occurring at the active site in the heterogeneous Ziegler−Natta catalytic systems. To model the catalyst, we considered the hypothetical species Mg_2Cl_6Ti−alkyl, the oxidation number of the Ti atom being III. For this system, we studied the insertion reaction of an ethylene molecule both on (i) a Ti−CH_3 bond and (ii) a Ti−CH_2CH_3 bond. We further considered the following termination reactions: (iii) β-hydrogen transfer to the metal; (iv) β-hydrogen transfer to the monomer; (v) C−H σ-bond activation. These reactions are shown in Scheme 1. In all the calculations, the density functional theory approach has been employed. This technique, which has emerged in the last few years as a powerful tool for the investigation of organometallic reactions, has been extensively applied to the study of olefin polymerizations with group 4 homogeneous metallocenes[2e,h−k,10] as well as with Ni-based homogeneous systems.[11]

Model and Computational Details

The considered Mg_2Cl_6Ti(alkyl)(alkene) system is the simplest model representative of the heterogeneous catalytic system composed by $TiCl_3$ supported on $MgCl_2$ (Figure 1). It is composed of a single Ti(III) atom octahedrally coordinated. Four coordination positions are occupied by Cl atoms, which represent the bridges which connect the Ti atom to the Mg atoms. A pendent Cl atom is bonded to each of the Mg atoms to saturate the valences. The two other coordination positions at the Ti atom are at the disposal of coordination of an alkyl group and of the monomer. In all the calculations, the geometry of the Mg_2Cl_6Ti skeleton has been treated as follows: the geometry around the Mg atoms and the bond lengths Ti−Cl and Mg−Cl have always been optimized. Differently, the Cl−Ti−Cl angles were fixed to 90°, and the two rings formed by the Ti atom, the Mg atom, and the two bridging Cl atoms were constrained to be planar. Finally, the dihedral angle between the four-membered rings was fixed at 90°. This corresponds to the simplifying assumption that the atoms on the surface present a structure close to that present in the bulk of the crystal. A different approach could consider a total relaxing of all the degrees of freedom. However, due to the small dimensions of the considered cluster, we think that this last approach would

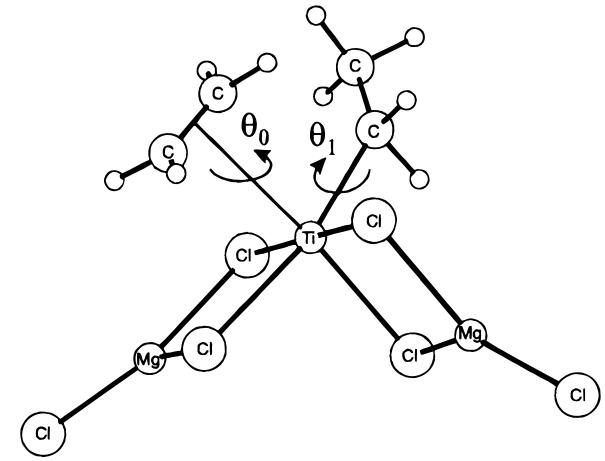

Figure 1. Schematic drawing of a model including an ethylene molecule and an ethyl group bonded to the Ti atom. The main internal coordinates that have been considered in the analysis are indicated. The sketched conformation correspond to $\theta_0 \approx 0°$ and $\theta_1 \approx -60°$.

(9) (a) Chien, J. C. W.; Wu, J.-C.; Kuo, C.-I. *J. Polym. Sci., Polym. Chem. Ed.* **1982**, *20*, 2019. (b) Chien, J. C. W.; Wu, J.-C.; Kuo, C.-I. *J. Polym. Sci., Polym. Chem. Ed.* **1982**, *20*, 2461.

(10) (a) Woo, T.; Fan, L.; Ziegler, T. *Organometallics* **1994**, *13*, 2252. (b) Lohrenz, J. C. W.; Woo, T. K.; Ziegler, T. *J. Am. Chem. Soc.* **1995**, *117*, 12793. (c) Margl, P. M.; Lohrenz, J. C. W.; Blöchl, P. E.; Ziegler, T. *J. Am. Chem. Soc.* **1996**, *118*, 4434. (d) Woo, T. K.; Margl, P. M.; Ziegler, T.; Blöchl, P. E. *J. Am. Chem. Soc.*, in press.

(11) (a) Musaev, D. G.; Froese, R. D. J.; Svensson, M.; Morokuma, K. *J. Am. Chem. Soc.* **1997**, *119*, 367. (b) Deng, L.; Margl, P. M.; Ziegler, T. *J. Am. Chem. Soc.* **1997**, *119*, 1094. (c) Deng, L.; Woo, T. K.; Cavallo, L.; Margl, P. M.; Ziegler, T. *J. Am. Chem. Soc.* **1997,** *119*, 6177.

imply deformations that would not be representative of the rearrangements that occur on the $MgCl_2$ surface.

In our model, the Ti atom is bridge-bonded to the two Mg atoms through two pairs of Cl atoms. Due to the presence of these bidentate chelating agents, the geometry of coordination at the Ti atom is chiral, and can be denoted as Δ or Λ according to IUPAC rules for chiral octahedral compounds.[12,13] As remarked by molecular mechanics studies,[13b] the chirality of this simplified model site is not sufficient to ensure stereospecificity during polymerization. However, all the models we have considered are of Δ chirality.

For the sake of consistency with the molecular mechanics models we developed for the stereospecificity for both the heterogeneous[13] and the homogeneous[14] Ziegler−Natta systems, we used the geometrical parameters defined in Figure 1 to characterize the obtained geometries. These are the dihedral angle θ_0 associated with the rotations of the olefin around the axis connecting the metal to the center of the double bond and the internal rotation angle θ_1 associated with the rotations around the bond between the Ti atom and the first carbon atom of the growing chain. At $\theta_0 \approx 0°$, the double bond of the olefin is aligned with the Ti−C(alkyl) σ bond. $\theta_1 \approx 0°$ corresponds to the conformation having the first C−C bond of the growing chain eclipsed with respect to the axis connecting the metal atom to the center of the double bond of the olefin.

The density functional calculations were carried out by using the HFS-LCAO package ADF, developed by Baerends et al.[15] The geometry optimization procedure has been developed by Versluis and Ziegler.[16] The electronic configurations of the systems were described by an uncontracted triple-ζ STO basis set on Ti (3s,3p,3d,4s,4p) and Mg (3s,3p,3d). Double-ζ STO basis sets were used for Cl (3s,3p), C (2s,2p), and H (1s). These basis sets[17] were augmented with single 3d and 2p polarization functions for the Cl, C, and H atoms, respectively.[17] The $1s^2$-$2s^22p^6$ configuration on Ti, Mg, and Cl and the $1s^2$ configuration on C were treated by the frozen-core approximation.[18] All the calculations have been performed by using the local potential by Vosko et al.,[19] augmented, also during the geometry optimizations, by the nonlocal corrections of Becke[20] and Perdew.[21] Due to the open-shell character of the systems under study, an unrestricted formalism has been used. To confirm the character of the stationary points as minima or transition states, frequency calculations were performed to check for the absence of negative eigenvalues and the presence of only one for the transition states. In the frequency calculations, the Mg_2Cl_6Ti skeleton was completely frozen to save computer time.

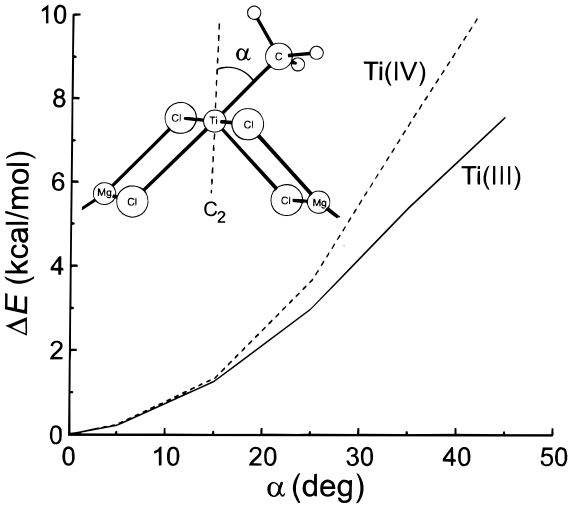

Figure 2. Plot of the total energy of the $Mg_2Cl_6Ti^{III}CH_3$ system, continuous line, and of the $[Mg_2Cl_6Ti^{IV}CH_3]^+$ system, dashed line, as a function of the angle α, formed by the Ti−C σ bond with the local C_2 symmetry axis.

Results and Discussion

Active Methyl Species Structure. Figure 2 plots the total energy of the $Mg_2Cl_6TiCH_3$ system as a function of the angle α, formed by the Ti(III)−C σ bond with the local C_2 symmetry axis. For the model of the heterogeneous catalyst we considered, the preferred orientation of the Ti(III)−C σ bond is clearly along the local symmetry axis, and the minimum energy geometry is a distorted trigonal bipyramid with the CH_3 group in the equatorial plane. To force the Ti−C bond to occupy an octahedral position is energetically costly ($\alpha = 45°$, $\Delta E = 7.6$ kcal/mol). For the analogous homogeneous $[Cp_2ZrCH_3]^+$ and $[CpSiH_2NHTiCH_3]^+$ systems, Ziegler and co-workers found that the preferred orientation of the Mt−C σ bond is not along the local symmetry axis.[10a] A shallow energy minimum (less than 3 kcal/mol) is found at $\alpha = 53°$ and 61°, respectively, whereas for the neutral Ti(III) $CpSiH_2NHTiCH_3$ system, this angle is noticeably reduced ($\alpha = 25°$). This difference in the degree of bending between neutral and cationic species was already pointed out by Bierwagen et al.[22] To further investigate this aspect, we changed the oxidation state of Ti from III to IV and we calculated the energy of the $[Mg_2Cl_6TiCH_3]^+$ system as a function of the angle α. The preference for a trigonal bipyramidal geometry is even enhanced for the Ti(IV) system, and thus, our findings do not depend on the metal oxidation state. Similar results were obtained by Clementi et al.,[8d] Sakai,[3e] and Jensen et al.[3f]

Insertion into a Ti−CH_3 Bond. The coordination of an ethylene molecule to **1** occurs without an energy barrier and leads to **2**, which lies 7.3 kcal/mol below **1**. The preferred orientation of the olefin is at $\theta_0 \approx 90°$, the C atoms of the olefin are slightly

(12) Nomenclature Of Inorganic Chemistry. *Pure Appl. Chem.* **1971**, *28*, 1.

(13) (a) Corradini, P.; Barone, V.; Fusco, R.; Guerra, G. *Eur. Polym. J.* **1979**, *15*, 133. (b) Corradini, P.; Barone, V.; Fusco, R.; Guerra, G. *J. Catal.* **1982**, *77*, 32. (c) Corradini, P.; Barone, V.; Guerra, G. *Macromolecules* **1982**, *15*, 1242. (d) Corradini, P.; Barone, V.; Fusco, R.; Guerra, G. *Gazz. Chim. Ital.* **1983**, *113*, 601. (e) Venditto, V.; Corradini, P.; Guerra, G.; Fusco, R. *Eur. Polym. J.* **1991**, *27*, 45.

(14) (a) Corradini, P.; Guerra, G.; Vacatello, M.; Villani, V. *Gazz. Chim. Ital.* **1988**, *118*, 173. (b) Cavallo, L.; Corradini, P.; Vacatello, M. *Polym. Commun.* **1989**, *30*, 236. (c) Venditto, V.; Guerra, G.; Corradini, P.; Fusco, R. *Polymer* **1990**, *31*, 530. (d) Cavallo, L.; Corradini, P.; Guerra, G.; Vacatello, M. *Polymer* **1991**, *32*, 1329. (e) Cavallo, L.; Corradini, P.; Guerra, G.; Vacatello, M. *Macromolecules* **1991**, *24*, 1784. (f) Cavallo, L.; Guerra, G.; Corradini, P.; Vacatello, M. *Chirality* **1991**, *3*, 299. (g) Guerra, G.; Cavallo, L.; Moscardi, G.; Vacatello, M.; Corradini, P. *J. Am. Chem. Soc.* **1994**, *116*, 2988. (h) Guerra, G.; Cavallo, L.; Moscardi, G.; Vacatello, M.; Corradini, P. *Macromolecules* **1996**, *29*, 4834. (i) Guerra, G.; Longo, P.; Cavallo, L.; Corradini, P.; Resconi, L. *J. Am. Chem. Soc.* **1997**, *119*, 4394.

(15) (a) Baerends, E. J.; Ellis, D. E.; Ros, P. *Chem. Phys.* **1973**, *2*, 41. (b) te Velde, G.; Baerends, E. J. *J. Comput. Phys.* **1992**, *99*, 84. (c) ADF 2.0.0 and 2.1.0, Vrije Universiteit Amsterdam, Amsterdam, The Netherlands, 1996.

(16) Versluis, L.; Ziegler, T. *J. Chem. Phys.* **1988**, *88*, 322.

(17) (a) Snijders, J. G.; Vernooijs, P.; Baerends, E. J. *At. Nucl. Data Tables* **1981**, *26*, 483. (b) Vernooijs, P.; Snijders, J. G.; Baerends, E. J. *Slater Type Basis Functions for the whole Periodic System*; Vrije Universiteit Amsterdam: Amsterdam, 1981.

(18) Baerends, E. J. Ph.D. Thesis, Vrije Universiteit Amsterdam, Amsterdam, 1975.

(19) Vosko, S. H.; Wilk, L.; Nusair, M. *Can. J. Phys.* **1980**, *58*, 1200.

(20) Becke, A. *Phys. Rev. A* **1988**, *38*, 3098.

(21) (a) Perdew, J. P. *Phys. Rev. B* **1986**, *33*, 8822. (b) Perdew, J. P. *Phys. Rev. B* **1986**, *34*, 7406.

(22) Bierwagen, E. P.; Bercaw, J. E.; Goddard, W. A., III. *J. Am. Chem. Soc.* **1994**, *116*, 1481.

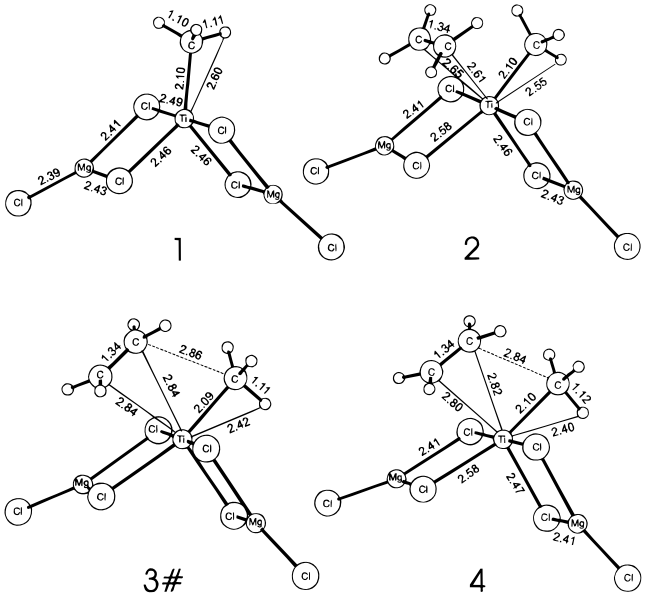

asymmetrically coordinated (2.61 and 2.65 Å), and a weak α-agostic interaction (2.55 Å) of the CH_3 group with the metal is present. Prior to insertion, rotation of the olefin to have the C−C double bond almost collinear with the Ti−CH_3 σ bond occurs through the transition state **3#** with $\theta_0 \approx 10°$ (3.5 kcal/mol above **2**) and leads to **4** with $\theta_0 \approx 0°$ (3.3 kcal/mol above **2**). As indicated by the larger Ti−C(olefin) distances (2.80 and 2.82 Å), the coordination of the olefin with $\theta_0 \approx 0°$ is slightly weakened with respect to **2**, while the α-agostic interaction of the CH_3 group with the metal is slightly strengthened (2.40 Å). Finally, the reverse process, which is from **4** to **2**, occurs with a negligible barrier (0.2 kcal/mol).

By shrinking the methyl−ethylene distance, the insertion of the olefin into the Ti−CH_3 bond occurs through the transition state **5#**, which lies 5.3 kcal/mol above **4**. The insertion process is stabilized by a remarkable α-agostic interaction (2.08 Å). Considering the low barrier for the reaction **4** → **2**, we think that the overall insertion barrier corresponds to the energy of the transition state **5#** relative to the π-complex **2** (8.6 kcal/mol). The kinetic insertion product **6** is obtained by relaxing the transition state **5#** on the product side and presents a weak γ-agostic interaction (2.61 Å). Structure **6** lies 14.6 kcal/mol below **2** and can rearrange through the transition state **7#** and a low barrier (0.3 kcal/mol) to the thermodynamic product **8**, 20.3 kcal/mol below **2**, which presents a strong β-agostic interaction (2.03 Å). The overall energy profile is reported in Figure 3 and corresponds to the lower curve (continuous line).

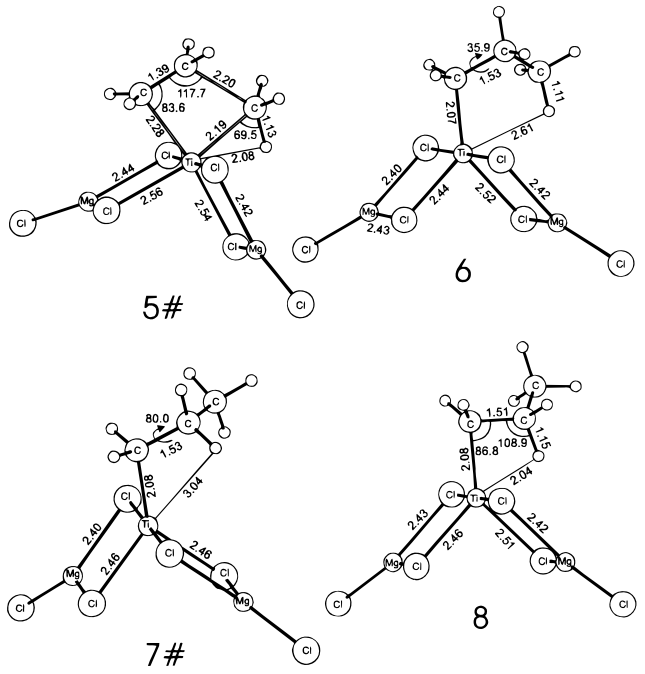

We also investigated the insertion reaction in which the H atoms of the methyl group are staggered with respect to the atoms bonded to the olefin C atom that is going to form the new C−C bond. With this aim, we calculated structures **2b**, **3#b**, **4b**, and **5#b**, which essentially differ from **2**, **3#**, **4**, and **5#** only by a rotation of 60° of the methyl group. The reaction path is approximately 1 kcal/mol higher than the one with an eclipsed conformation of the methyl group. This is probably due to the absence of the stabilizing α-agostic interaction. The energy profile is reported in Figure 3 (dashed line), and the activation barrier, calculated as the energy difference between **5#b** and **2b**, is equal to 9.5 kcal/mol. Since this last reaction path does not correspond to the lowest energy profile, we did not characterize the structures along it, either as minima or transition states, through frequency calculations.

Propagation Step. According to our model, the propagation step should start from the β-agostic stabilized structure **8**. However, to save computer time, we replaced the *n*-propyl group with an ethyl group. Thus, the β-agostic stabilized structure **9** represents the resting state of the propagation step. Coordination of an ethylene molecule to **9** can occur from the Ti−C σ bond side as well as from the β-agostic bond side. The first of these two attacks proceeds in a barrierless fashion and leads to **10**, which lies 1.8 kcal/mol below **9**. As for the insertion on a Ti−

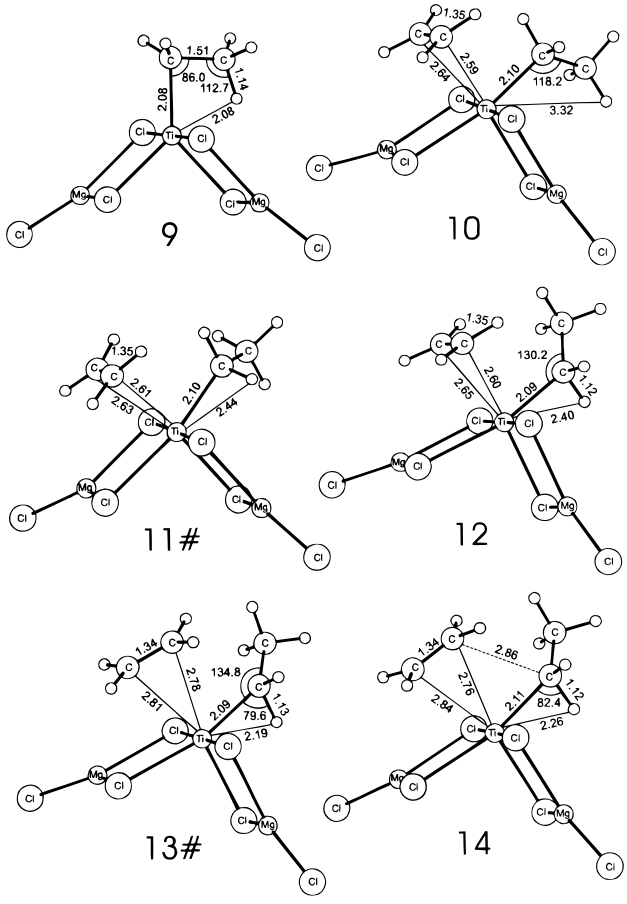

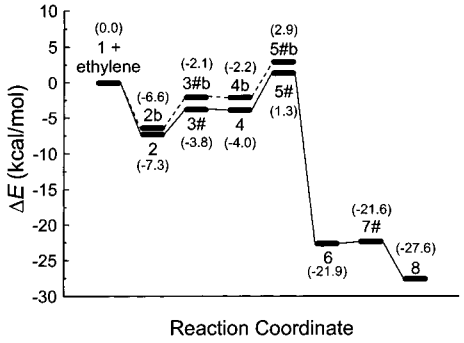

Figure 3. Energy diagram for the insertion of ethylene into a Ti−CH_3 σ bond. Symbols 1−8 correspond to structures 1−8 described in the text.

CH_3 bond, the preferred coordination of the olefin corresponds to $\theta_0 \approx 90°$. The β-agostic interaction of the growing chain with the Ti atom is completely removed during the coordination, while the Ti−C σ bond shifts from the local symmetry axis to an octahedral coordination position. After the ethylene coordination, the torsional angle θ_1 that describes the orientation of the growing chain relative to the monomer is defined and it assumes a value close to 180°. The subsequent insertion reaction can proceed in two different fashions. The first path we explored begins with a rearrangement of the growing chain to assume a conformation, which facilitates the insertion step. This rearrangement proceeds through the transition state **11#** with $\theta_1 \approx -120°$ (0.5 kcal/mol above **10**) and leads to **12** with $\theta_1 \approx -40°$ (1.1 kcal/mol below **10**), which presents a weak α-agostic interaction (2.40 Å). Prior to insertion, rotation of the olefin occurs through the transition state **13#** with $\theta_0 \approx -20°$ (3.9 kcal/mol above **12**) and leads to **14** with $\theta_0 \approx 0°$ (3.6 kcal/mol above **12**). The coordination of the olefin with $\theta_0 \approx 0°$ is slightly weakened (Ti−C(olefin) distances = 2.76 and 2.84 Å), and the value assumed by θ_1 is close to −60°.

The olefin insertion into the Ti−C σ bond occurs through the transition state **15#**, which lies 3.0 kcal/mol above **14**. This reaction is facilitated by a remarkable α-agostic interaction and leads to the γ-agostic kinetic product **16** (14.9 kcal/mol below **12**). Considering the low barrier that separates **14** from **12**, the overall insertion barrier corresponds, in our opinion, to the energy of the transition state **15#** with respect to **12**, which amounts to 6.6 kcal/mol. The γ-agostic product **16** can rearrange through the transition state **17#** and a low barrier (0.8 kcal/mol) to the thermodynamic product **18** (22.3 kcal/mol below **12**), which presents a strong β-agostic interaction. The position of the growing chain in **18** is the same as that in **9**. Let us recall, instead, that for analogous models developed for the homogeneous systems, the growing chain at the end of two successive insertion steps occupies two different coordination positions.[2,10] As discussed in detail in the last section, this has remarkable influences on the stereospecificity of the model complexes. The overall energy profile is reported in Figure 4 and corresponds to the lower curve (continuous line).[23]

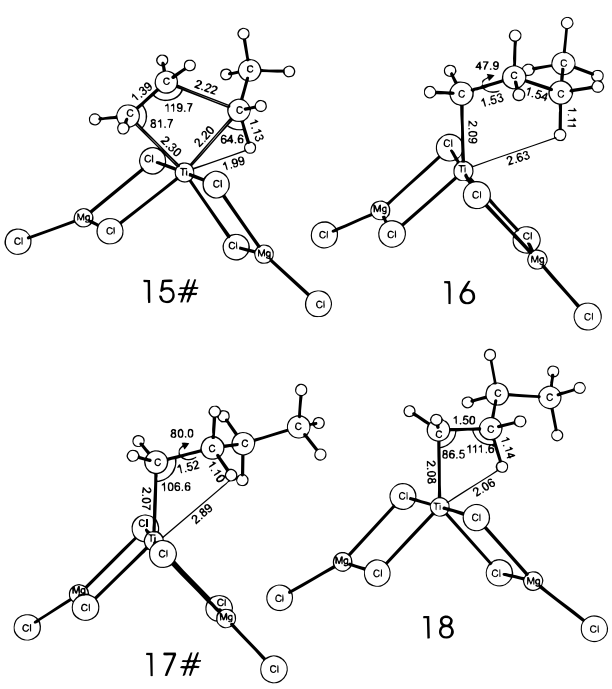

The alternative insertion mechanism we considered occurs without the rearrangement of the growing chain from values of $\theta_1 \approx 180°$ to values of $\theta_1 \approx \pm 60°$ prior to insertion (dashed line in Figure 4). In this case, starting from **10**, the olefin rotates to arrive at the minimum energy structure **14b** with $\theta_0 \approx 0°$ (4.2 kcal/mol above **10**). The corresponding insertion reaction proceeds through the transition state **15#b**, with an activation barrier of 14.6 kcal/mol. The four-center transition state **15#b** is probably destabilized by steric interactions with the chlorine atoms, which also prevent the formation of stabilizing agostic interactions. A rearrangement of the atoms at the catalyst surface could partially relax these interactions. For this reason, the calculated barrier is probably overestimated. However, according to our model, the insertion with $\theta_1 \approx \pm 60°$ is remarkably favored relative to the insertion with $\theta_1 \approx 180°$ ($\Delta\Delta E^{\#} = 8.0$ kcal/mol). Thus, we think that no reasonable rearrangement at the catalyst surface can modify our conclusions.

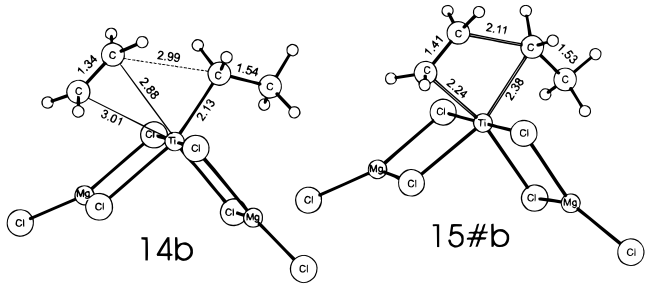

To distinguish between the two orientations of the growing chain in the insertion reaction for the homogeneous systems, Ziegler and co-workers coined the terms "frontside" and "backside" insertions, which correspond to transition states for the insertion reaction with values of $\theta_1 \approx \pm 60°$ and $\theta_1 \approx 180°$, respectively. Also for the systems they considered, the $\Delta\Delta E^{\#}$ is always in favor of the frontside insertion ($\theta_1 \approx \pm 60°$), although the $\Delta\Delta E^{\#}$ values for the homogeneous systems are noticeably smaller (2.8 and 3.4 kcal/mol for the systems $[Cp_2ZrR]^+$ and $[CpSiH_2NHTiR]^+$).[10b,c] Differently from the octahedral heterogeneous systems, for the pseudotetrahedral homogeneous systems, the in-plane orientation of the olefin and of the first two C atoms of the growing chain in the transition state for the insertion with $\theta_1 \approx 180°$ nicely accommodates into the metallocene equatorial belt. Moreover, the presence of a β-agostic interaction of the growing chain probably stabilizes the transition state. The clear preference for insertion paths with

(23) Despite their chirality, for the simplified models considered in this paper, the structures energetically equivalent to **11#**, **12**, **13#**, **14**, and **15#** are obtained by inverting the signs of the θ_0 and θ_1 torsional angles, that is, positive values for both θ_0 and θ_1.

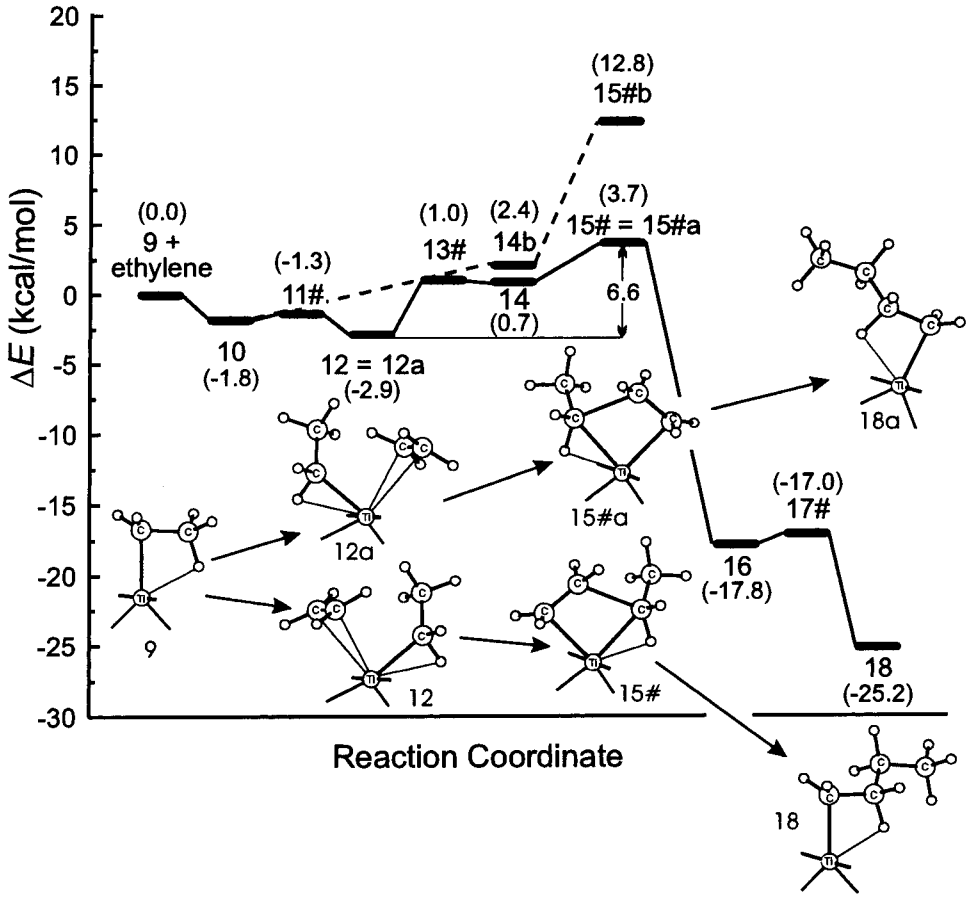

Figure 4. Energy diagram for the propagation reaction corresponding to the insertion of ethylene into a Ti−CH_2CH_3 σ bond. Symbols 9−18 correspond to structures **9**−**18** described in the text. Schematic sketches of the most important structures characterizing the reaction paths derived from the monomer attack from the Ti−C σ bond side (**9**, **12**, **15#**, and **18**) as well as from the β-agostic bond side (**9**, **12a**, **15#a**, and **18a**) are reported.

$\theta_1 \approx \pm 60°$ for Ziegler−Natta catalysts is also a strong support to the molecular mechanics studies on the stereospecificity of both heterogeneous[13] and homogeneous[14] systems, which are based on the concept of the "chiral orientation of the growing chain", which implies values of $\theta_1 \approx \pm 60°$.

As for the second channel for the olefin attack to the metal atom of structure **9**, that is, from the β-agostic bond side, the coordination occurs through a concerted mechanism which implies a rotation of the ethyl group around the Ti−C σ bond with a disruption of the β-agostic interaction. Due to the flatness of the potential energy surface, we did not attempt a transition state search, but according to our scanning, the monomer coordination occurs with an almost negligible barrier (<1 kcal/mol) and leads to a structure with $\theta_1 \approx -40°$ and $\theta_0 \approx 90°$. This structure has the same θ_1 and θ_0 values of **12**, but the relative coordination positions of the growing chain and of the monomer are exchanged. Due to the presence of the local C_2 symmetry axis, the two coordination positions available to the chain and to the monomer are homotopic, and thus, the minimum energy geometry obtained from the olefin attack from the β-agostic bond side is equivalent to structure **12**. For this reason, the propagation reaction can be considered to proceed from **12** along the already discussed path. Considering the substantial absence of barrier for the two coordination channels of the olefin, we think that the monomer attack to the metal atom does not have a preferential path. Schematic sketches of the most important structures characterizing the reaction paths deriving from the monomer attack from the Ti−C σ-bond side (**9**, **12**, **15#**, and **18**) as well as from the β-agostic bond side (**9**, **12a**, **15#a**, and **18a**) are reported in Figure 4.

Transfer to the Metal. The first termination reaction considered is the β-hydrogen transfer to the metal. Starting from the β-agostic propyl structure **8**, we elongated the β-agostic C−H bond up to the transition state **19#**, with a C−H distance of 2.76 Å, and a value of the forming $\theta_0 \approx -60°$. The product

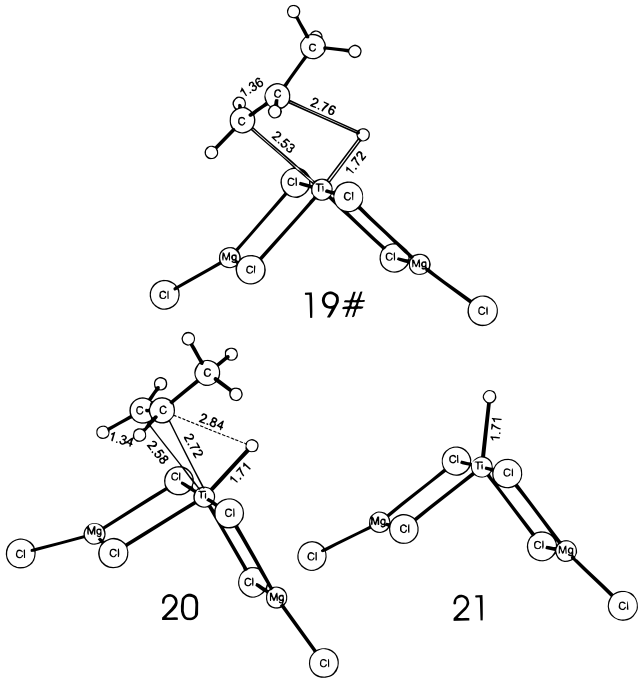

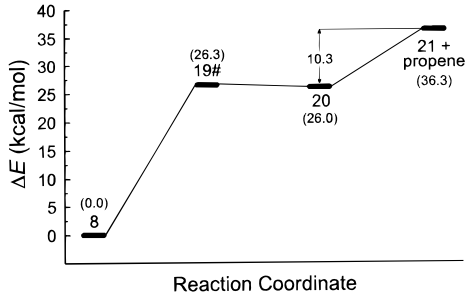

Figure 5. Energy diagram for the termination reaction corresponding to the β-hydrogen transfer to the metal. Symbols 8−21 correspond to structures **8**−**21** described in the text.

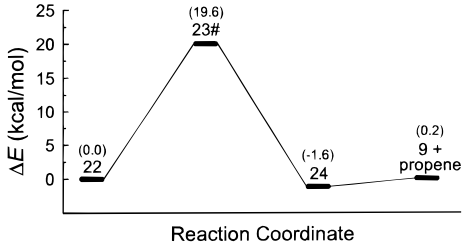

Figure 6. Energy diagram for the termination reaction corresponding to the β-hydrogen transfer to the monomer. Symbols 22−24 correspond to structures **22**−**24** described in the text.

20 presents a Ti−H adduct with a propene-coordinated molecule with $\theta_0 \approx -90°$. The calculated barrier for the transfer to the metal is 26.3 kcal/mol. The energy of coordination of the propene in **20** is 10.3 kcal/mol, and the final product of the β-hydrogen transfer to the metal is the Ti−H adduct **21**, from which the growth of a new chain can be started. The overall energy profile is reported in Figure 5.

Transfer to the Monomer. The starting point for the termination reaction that involves the transfer of a β hydrogen of the growing chain to the monomer is the π complex **22**, with

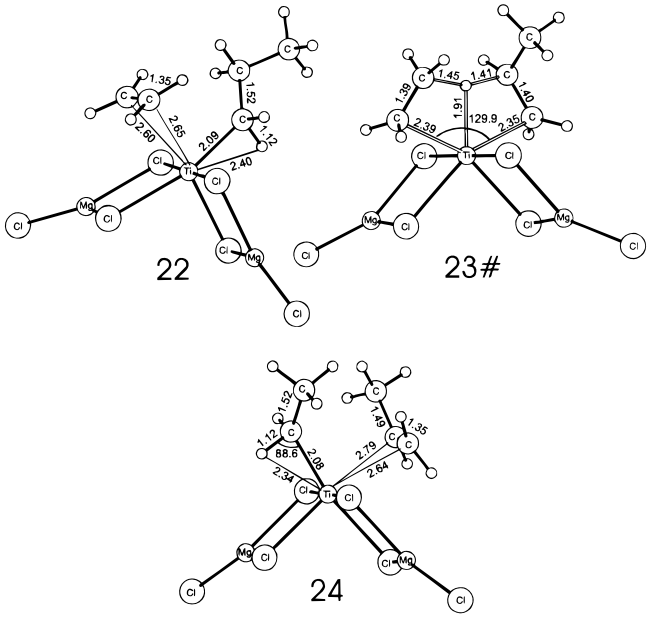

$\theta_0 \approx 90°$ and $\theta_1 \approx -40°$. Shrinking the distance between one of the β hydrogens of the propyl group with a carbon atom of the ethylene molecule brings the transition state **23#**, with an activation barrier of 19.6 kcal/mol. Relaxing the transition state on the product side yields structure **24**, which presents an ethyl group σ-bonded to the metal, and a π-coordinated propene molecule that represents the vinylic chain end. The final product is the β-agostic ethyl complex **9**, from which the growth of a new chain can be started. The corresponding energy profile is reported in Figure 6.

As for the homogeneous systems, the H transfer is assisted by the metal. The C−H distances in **23#** (1.41 and 1.45 Å) are noticeably shorter than the corresponding distances (≈1.50 Å) in the transition state for the β-hydrogen transfer to the monomer for the homogeneous system $[CpSiH_2NHTiR]^+$.[10d] This reaction, which is of relatively low energy for the homogeneous systems (<10 kcal/mol), is of remarkable energy. As for the insertion reaction with $\theta_1 \approx 180°$, the different coordination at the metal atom (octahedral vs tetrahedral) completely changes the space at the disposal of the reacting atoms. Thus, a rearrangement of the atoms at the catalyst surface could partially relax the steric interactions occurring in the transition state. For this reason, the calculated barrier is probably overestimated.

C−H σ-Bond Activation. Another termination reaction that has been considered involves the activation of a C−H σ bond of the monomer. From the π complex **12**, we shrunk the distance between the C_α of the growing chain and one of the hydrogen atoms of the monomer. The transition state for this reaction, **25#**, lies 21.3 kcal/mol above **12**. The C−H σ-bond

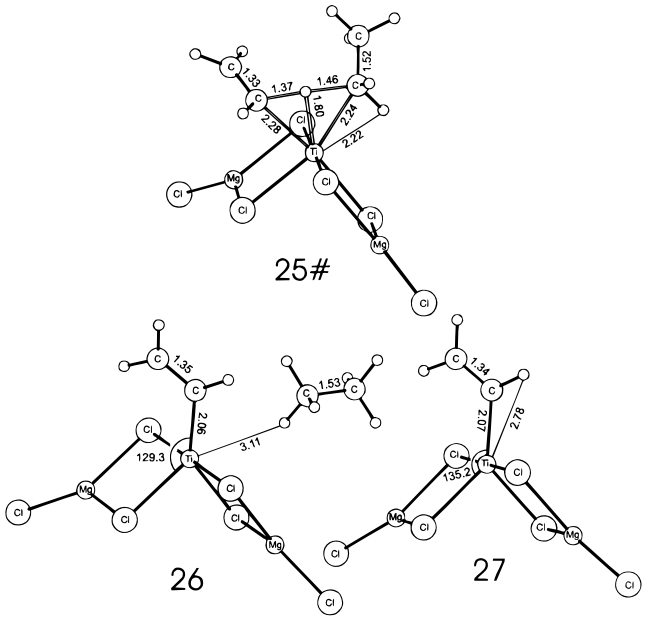

activation is facilitated by a strong interaction between the H atom that is going to be transferred and the metal atom, as indicated by the short Ti−H distance in the transition state **25#** (1.80 Å). The direct product **26** presents a vinylidene moiety bound to the metal and a weakly coordinated ethane molecule. The energy of coordination of the alkane group amounts to 0.6 kcal/mol only. The overall energy profile is reported in Figure 7, and **27** represents the final structure, after the detachment of the ethane molecule. The Ti−C distance in **27** is equal to 2.07 Å, and the Ti−C bond lies along the local symmetry axis.

Comparison with Experimental Results. The main results obtained in the present study are in fair agreement with several experimental facts. The calculated barrier for the propagation reaction is $\Delta E^{\#} = 6.6$ kcal/mol, and the inclusion of zero-point vibrational energy contributions, ZPE, slightly increases the calculated barrier ($\Delta E^{\#}_{ZPE} = 7.3$ kcal/mol). This value is in reasonable agreement with the value of the activation energy determined for propene polymerization with supported catalysts

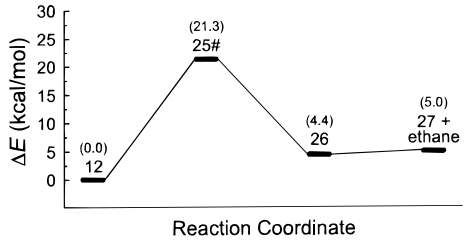

Figure 7. Energy diagram for the termination reaction corresponding to the C−H σ bond activation. Symbols 12−27 correspond to structures **12**−**27** described in the text.

($\Delta E^{\#} \approx 9.5-12.0$ kcal/mol).[24] Considering that the activation energy data relative to chain propagation are only available for the polymerization of 1-butene with unsupported $TiCl_3$-based systems (4.5 kcal/mol),[25] we checked the performance of our approach by calculating the activation energy for the catalytic model system in which the Mg_2Cl_6Ti part has been replaced with the Ti_3Cl_8 part. The calculated activation energy ($\Delta E^{\#} =$ 4.8 kcal/mol) can be directly compared with the experimental data, and it is in excellent agreement with it.

All the considered termination reactions (transfer to the metal or to the monomer, C−H σ-bond activation) present activation barriers noticeably higher ($\Delta E^{\#} =$ 26.3, 19.6, and 21.3 kcal/mol, respectively). Inclusion of ZPE contributions decreases the calculated barrier by ca. 2 kcal/mol ($\Delta E^{\#}_{ZPE} =$ 23.4, 18.0, and 18.9 kcal/mol). This is in agreement with the very high molecular weights ($>10^6$) obtained with the heterogeneous catalysts. In agreement with the experimental findings,[1b,c] the transfer to the monomer is favored with respect to the β-hydrogen transfer to the metal.

The difference between the activation barrier of the most favored termination reaction and the propagation reaction, $\Delta\Delta E^{\#} =$ 13.0 kcal/mol, is noticeably higher than the value that can be calculated on the basis of the observed molecular weights (ca. 7 kcal/mol). Inclusion of ZPE ($\Delta\Delta E^{\#}_{ZPE} =$ 10.7 kcal/mol) remarkably reduces the disagreement between the calculated and the experimentally observed values. Moreover, as discussed in a previous section, the activation barrier for the β-hydrogen transfer to the monomer is somewhat overestimated. A better approximation to this activation barrier could probably lead to a better agreement.

Position of the Growing Chain after Monomer Insertion and Stereospecificity. The position of the growing chain after each monomer insertion, that is, the angle α formed by the Ti−C σ bond with the local symmetry axis (see Figure 2), is extremely relevant for the polymerization mechanism and, in consequence, for the stereospecificity of the proposed model complexes, both for heterogeneous and for homogeneous catalytic systems.

The calculated energy minima of $\alpha \approx 60°$ for metallocene-based model complexes[10a,26] has contributed to the rationalization of the regular **chain migratory insertion mechanism** for olefin polymerizations. This mechanism implies a migration of the growing chain to the coordination position previously occupied by the monomer at each insertion step. It is essential to rationalize the syndiospecific behavior of metallocene complexes with local C_s symmetry, whose monomer coordination positions are enantiotopic and hence of opposite enantioselectivity.[14e,27] This mechanism has been definitely proved by the hemiisospecific behavior of C_1 symmetric metallocene complexes when only one of the two monomer coordination positions is enantioselective.[14e,28]

Chart 1

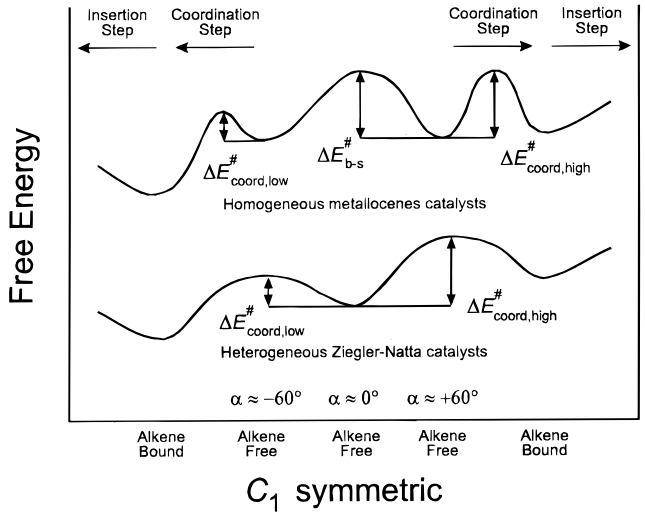

However, several experimental facts[29] and molecular modeling studies[14h] indicate that the chain migratory insertion mechanism does not operate regularly for C_1 symmetric metallocene catalysts when the activation energies for monomer coordination in the two available positions are energetically nonequivalent. In fact, in the alkene-free state, the growing chain can move to the previously occupied coordination position (back-skip of the growing chain) before coordination of a new monomer molecule, eventually leading to the minimum energy alkene-bound intermediate. As sketched in the upper part of Chart 1, the probability of occurrence of a back-skip of the chain in the alkene-free state of the metallocene catalytic complexes is dependent on the difference between the activation energy for the chain back-skip ($\Delta E^{\#}_{b-s}$) and the activation energy for the formation of the high-energy alkene-bound intermediate ($\Delta E^{\#}_{coord,high}$). Of course, the frequency of back-skip of the chain can be substantially increased by the reduction of the monomer concentration.[29]

According to the present calculations, a regular chain migratory mechanism for the proposed models for the heterogeneous Ziegler−Natta catalysts seems unlikely. In fact, the chain orients itself along an axis that is intermediate between the two available octahedral coordination positions ($\alpha = 0°$) in the absence of the monomer molecule. A possible **nonmigratory insertion mechanism** has no consequences on the stereospecific behavior of heterogeneous catalytic models with local C_2 symmetry, as far as the two positions available for monomer coordination are homotopic. Thus, if the insertion step is enantioselective, irrespective of the coordination position, the same monomer enantioface would always be coordinated and inserted, producing isotactic polymers. Models with a local C_2 symmetry have been proposed by Allegra several years ago for the heterogeneous catalysis on $TiCl_3$.[30]

(24) (a) Keii, T.; Suzuki, E.; Tamura, M.; Murata, M.; Doi, Y. *Makromol. Chem.* **1982**, *183*, 2285. (b) Keii, T.; Terano, M.; Kimura, K.; Ishii, K. In *Transition Metals and Organometallics as Catalysts for Olefin Polymerization*; Kaminsky, W., Sinn, H., Eds.; Springer-Verlag: Berlin, 1988; p 3.

(25) Natta, G.; Zambelli, A.; Pasquon, G.; Giongo, G. M. *Chim. Ind. (Milan)* **1966**, *48*, 1298.

(26) Lauer, J. W.; Hoffmann, R. *J. Am. Chem. Soc.* **1976**, *98*, 1729.

(27) Ewen, J. A.; Jones, R. L.; Razavi, A.; Ferrara, J. D. *J. Am. Chem. Soc.* **1988**, *110*, 6255.

(28) Ewen, J. A.; Elder, M. J.; Jones, R. L.; Haspeslagh, L.; Atwood, J. L.; Bott, S. G.; Robinson, K. *Makromol. Chem., Macromol. Symp.* **1991**, *48/49*, 253.

(29) (a) Farina, M.; Di Silvestro, G.; Sozzani, P. *Macromolecules* **1993**, *26*, 946. (b) Rieger, B.; Jany, G.; Fawzi, R.; Steiman, M. *Organometallics* **1994**, *13*, 647.

(30) Allegra, G. *Makromol. Chem.* **1971**, *145*, 235.

For the case of nonmigratory insertion mechanism ($\alpha = 0°$) at catalytic sites with C_1 symmetry, the probability that the monomer coordination occurs to one or the other of the two coordination positions is directly related to the energy difference, if any, between the corresponding activation energies ($\Delta E^{\#}_{\text{coord,high}} - \Delta E^{\#}_{\text{coord,low}}$ in the lower part of Chart 1). If a substantial energy difference is present, the monomer coordination and insertion would occur substantially at a given coordination position only. In that case, the isospecificity would be related to the enantioselectivity of the insertion reaction corresponding to the minimum energy monomer coordination position only. Models of this type have been proposed by Cossee.[7a,c]

The enantioselectivity of both C_2 and C_1 symmetric model sites has been rationalized in terms of the chiral orientation of the growing chain mechanism by Corradini and co-workers.[13]

A comparison of the schematic energy profiles of Chart 1, suggests that for C_1 symmetric catalytic sites with $\Delta E^{\#}_{\text{coord,high}} - \Delta E^{\#}_{\text{coord,low}} > 3$ kcal/mol, the monomer coordination and insertion would occur essentially on the same octahedral coordination position for heterogeneous Ziegler−Natta catalytic models, whereas (due to the energy barrier for the chain backskip) the monomer coordination and insertion would be possible (although less probable) also at the position leading to higher energy intermediates for metallocene-based catalytic models.

As a final remark, it is worth noting that model sites with local C_s symmetry representing enantiotopic coordination positions are expected to be aspecific in the framework of a nonmigratory insertion mechanism, even if the insertion step is enantioselective.

Conclusions

In the present study, we considered the propagation as well as the termination reactions at catalytic site models of the classical heterogeneous Ziegler−Natta catalytic system. The considered species were of the type Mg_2Cl_6Ti−alkyl, the oxidation number of the Ti atom being III. Our study indicated that (i) the preferred orientation of the Ti−C(alkyl) bond in the absence of a coordinated olefin is along the local symmetry axis. To force this bond to occupy an octahedral coordination position is energetically quite costly (ca. 8 kcal/mol). (ii) The propagation reaction occurs in a stepwise fashion. It starts with the coordination of the olefin, and the most favored mechanism requires a rearrangement of the growing chain out of the four-center transition-state plane (values of $\theta_1 \approx = \pm 60°$ in our framework). The insertion reaction is facilitated by a α-agostic interaction, and the overall activation barrier, including ZPE contributions, is 7.3 kcal/mol. (iii) The most favored termination reactions involve a coordinated monomer. The β-hydrogen transfer to the monomer and the C−H σ-bond activation are of similar energy ($\Delta E^{\#}_{\text{ZPE}} = 18.0$ and 18.9 kcal/mol). Both of these reactions can be considered to begin from the same coordination intermediate, which leads to the propagation reaction. The other termination reaction considered, the β-hydrogen transfer to the metal, presents a higher activation barrier ($\Delta E^{\#}_{\text{ZPE}} = 23.4$ kcal/mol).

Acknowledgment. We thank Prof. V. Busico of the University of Naples and scientists of Montell Polyolefins for useful discussions and Dr. T. K. Woo of the University of Calgary for useful hints in using the ADF package. Financial support from the "Progetto Strategico Tecnologie Chimiche Innovative, Ministero dell′ Università e della Ricerca Scientifica e Tecnologica of Italy" and Montell Polyolefins is gratefully acknowledged.

JA972618N